Electrochemical behaviors of CuS as a cathode material for lithium secondary batteries

J.-S. Chung[a], H.-J. Sohn[b],*

[a]*Department of Mineral and Petroleum Engineering, Seoul National University, Seoul 151-742, South Korea*
[b]*School of Materials Science and Engineering, Seoul National University, Seoul 151-742, South Korea*

Abstract

Systematic studies of CuS as a cathode material for a Lithium rechargeable battery are performed in 1 M LiPF$_6$/EC-2EMC electrolyte. CuS undergoes a two-step reaction during the first discharge to 1.5 V with a capacity of 530 mAh^{-1} g. The voltage profile and X-ray diffraction (XRD) patterns of the discharge reactions show the formation of Li$_x$CuS during the first voltage plateau, and Cu$_{1.96}$S, Li$_2$S and metallic Cu during the second voltage plateau. The second plateau reactions are highly irreversible with partial dissolution of Li$_2$S in the electrolyte which causes poor cycleability. The cycleability can be much improved by limiting the potential window between 2.6 and 1.8 V. The capacity is maintained of more than 70% of the initial value over 60 cycles with a cycle efficiency of 99%. © 2002 Elsevier Science B.V. All rights reserved.

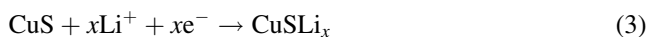*Keywords:* CuS; Cathode; Lithium rechargeable battery

1. Introduction

In lithium-ion secondary batteries, the capacity of the cathode material is generally much lower than that of the anode material. This is a main barrier for enhancing the specific energy of such batteries. Among the various candidates for cathode materials, sulfur and sulfur compounds are known to be good materials because of their high theoretical capacity.
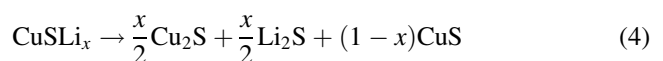
The Li/CuS system was a promising primary battery for high energy consumer electronics during the early stages of the development of lithium batteries [1–7]. This was because, CuS has a good electronic conductivity of 10^3 S^{-1} cm and a high energy capacity of 560 mAh^{-1} g [8–10]. The cathodic reactions of CuS occur sequentially as follows [5–7,11–13]:

$$2Li^+ + 2CuS + 2e^- \rightarrow Li_2S + Cu_2S \tag{1}$$

$$2Li^+ + Cu_2S + 2e^- \rightarrow Li_2S + 2Cu \tag{2}$$
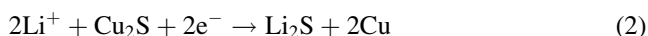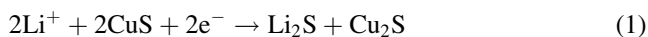
Later, it was proposed that the first step of the reaction consisted of the insertion of lithium-ions into the CuS crystal lattice when $x < 2$ [6,13,14], i.e.

$$CuS + xLi^+ + xe^- \rightarrow CuSLi_x \tag{3}$$

* Corresponding author. Tel.: +82-2-880-7226; fax: +82-2-885-9671.
E-mail address: hjsohn@snu.ac.kr (H.-J. Sohn).

followed by a fast disproportionation at moderate discharge where $x < 1$,

$$CuSLi_x \rightarrow \frac{x}{2}Cu_2S + \frac{x}{2}Li_2S + (1-x)CuS \tag{4}$$

The sequence of reactions (3) and (4) describe a stepwise process and Cu$_2$S formed by reaction (4) will subsequently discharge to copper and Li$_2$S at lower voltage according to reaction (2).

Several attempts had been made to use CuS as a cathode material for a rechargeable battery [15–17]. Hughes et al. [16] stated that the main problem of the Li/CuS secondary cell was a rapid drop in capacity. Exner and Hep [17] reported that an Li/CuS coin cell with a 1 M LiCF$_3$SO$_3$/ 1,3-dioxolane electrolyte gave only 50% charge capacity compared with the discharge capacity at a constant current. The same workers evaluated the rechargeability of the cell by cyclic voltametry at 5% depth-of-discharge (DoD) up to 1000 cycles, and concluded that the discharge reaction of cell was similar to Eq. (3) and insisted that there was no change in chemistry during cycling.

In this study, the use of CuS as a cathode material for a secondary lithium battery in liquid electrolyte is investigated, and the reaction mechanism during charge and discharge is studied with electrochemical techniques, X-ray diffractometry and spectroscopy. Also, a method to enhance the cycleability of the material is discussed.

2. Experimental

High purity CuS powders (over 99.99%, Aldrich) were used as received. Since impurities such as copper sulfates, copper thiosulfates, sulfur and moisture affect significantly the electrochemical performance of the CuS electrode [5–7], the samples were opened and kept in glove box to prevent contamination. KS-6 (Lonza) was used as a conductive carbon and polyvynilidene fluoride (PVDF, KYNAR 741; elf Atochem) was used as a binder. Both materials were vacuum dried for 2 days at 150 and 120 °C, respectively.

Cathode slurry was prepared by mixing cathode active material (72 wt.%), conductive carbon (18 wt.%) and binder (10 wt.%) in *n*-methyl pyrrolidinone (NMP). The homogeneously mixed slurry was coated on to an Ni foil (Inco Alloy: 10 μm thickness) current-collector using a doctor blade type coater (Mathis Lab-coater), and dried at 80 °C for 20 min. This was followed by vacuum drying at 80–85 °C for more than 48 h to remove completely any residual mixing solvent and volatile impurities. The dried cathode film was roll pressed and cut into discs of 1.3 cm diameter to serve as electrodes for coin cells. The weight of cathode active material per unit area was 6–7 mg cm^{-2}. All procedures were performed in dry room and glove box. The cell was fabricated by using lithium foil (Cyprus Foot Mineral: 150 μm) as an anode on a copper foil current-collector, a 20 μm thick porous polypropylene film (Cellgard No. 2400) as a separator, and an excess amount of electrolyte (1 M LiPF$_6$ in EC + 2EMC mixture, Mitsubishi Chemical Co., Battery grade).

The EVS test was conducted with a Maccor cycle tester by imposing a potential step (10 mV) at room temperature with a threshold current of 10 μA. X-ray diffraction (XRD) patterns were obtained with a diffractometer (Rigaku Geigerflex D/Max-III C) using Ni filtered Cu Kα radiation to identify the intermediate and final products formed at each

potential during charge and discharge at a rate of 0.02 mA/cm^2. Scanning electron microscopy (SEM) (JEOL JSM-840 A) was employed to examine changes in the morphology of the electrode. Changes in the composition of the anode during reactions were monitored using EDS. Samples were carried to the instrument in tightly sealed packs, and a glove bag (Aldrich) was attached to the mouth of the preparation chamber of each instrument to minimize contamination.

Since Li$_2$S is formed during discharge and Li$_2$S$_x$ ($x > 1$, lithium polysulfide) is known to dissolve in the electrolyte [18,19], ion chromatography (Dionex 100) was used to detect the sulfur or sulfur compounds by measuring sulfate ion (SO$_4^-$). Detailed procedures can be found elsewhere [20,21].

3. Results and discussion

The EVS diagram of the CuS electrode an the first cycle is shown in Fig. 1. It is seen that discharging reactions take place at 2.05 and 1.68 V, and that peaks for the charging reactions appear at 1.85 and 2.25–2.41 V. Although, the capacity of each peak (257 and 264 mAh^{-1} g) during the discharge reaction on the first cycle is approximately the same, the capacity of the higher voltage peak (350 mAh^{-1} g) during charging is much larger than that of the lower voltage one (21 mAh^{-1} g) during charge. The voltage profile for the five cycles is presented in Fig. 2. This shows that the discharge reaction consists of two-steps which correspond to two voltage plateaux. The charging reactions are rather complicated with several plateaux and will be discussed later. The first discharge capacity of the system is near to the theoretical value of 520 mAh^{-1} g (93.0% of theoretical capacity, 560 mAh^{-1} g) but the charge capacity declined to 370 mAh^{-1} g (66.0% of theoretical and 71% of discharge
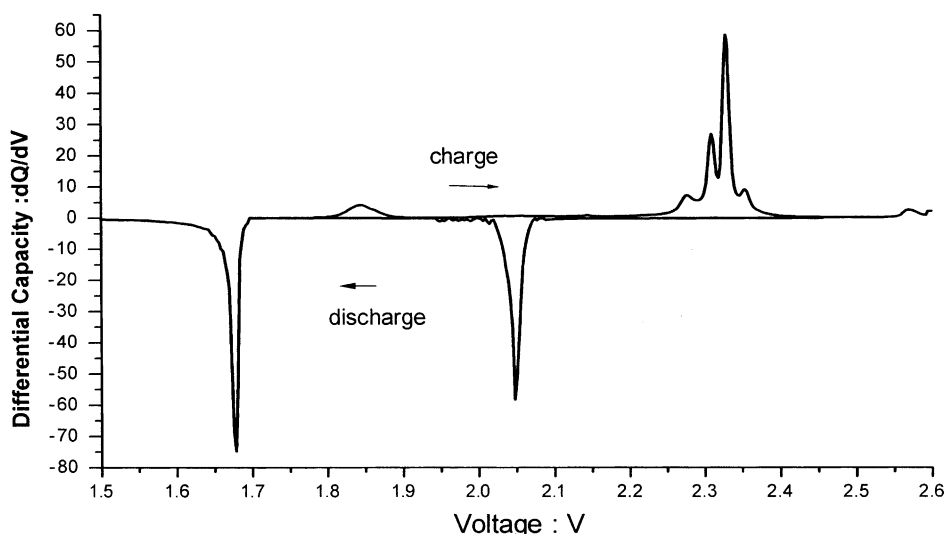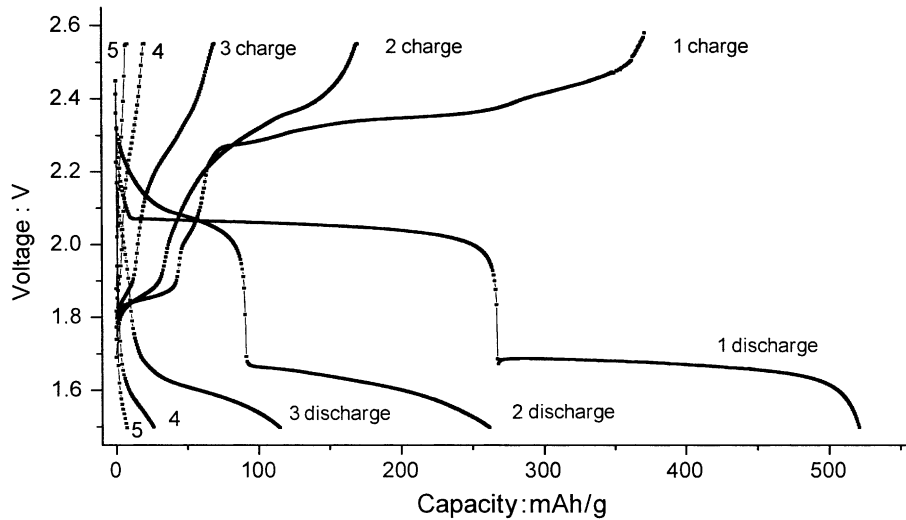

Fig. 1. EVS diagram of CuS electrode.

Fig. 2. Behaviors of high purity CuS electrode during five cycles between 1.5 and 2.6 V range at room temperature.
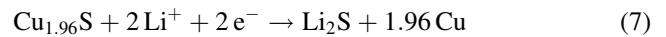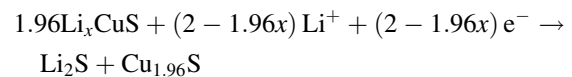
capacity, respectively). The first cycle cell behavior agrees well with the reported data [1–7,13,14].

The XRD patterns of the CuS electrode during the first cycle are shown in Fig. 3. The pattern does not change during discharge from the open circuit voltage (OCV) to 1.8 V (Fig. 3, curves (a)–(c)), which indicates that lithium is inserted into the CuS lattice as given by reaction (3) during the first voltage plateau, and retains the homogeneous Li_xCuS phase. The change of XRD pattern starts from 1.68 V which is the exact location of the second voltage plateau. As can be seen in Fig. 3 (d), the Bragg peaks of djurleite ($Cu_{1.96}S$), Li_2S and metallic Cu appear. When the voltage is lowered further to 1.5 V, which is below the second voltage plateau as shown in Fig. 2, only Li_2S and Cu peaks are present with a trace of $Cu_{1.96}S$, most of the $Cu_{1.96}S$ is changed to Li_2S and Cu. Based on the above facts, reactions occurring during discharge can be written as.

First plateau reaction:

$$CuS + xLi + xe^- \rightarrow Li_xCuS \tag{5}$$

Second plateau reactions occurring simultaneously, namely:

$$1.96Li_xCuS + (2 - 1.96x)\,Li^+ + (2 - 1.96x)\,e^- \rightarrow$$
$$Li_2S + Cu_{1.96}S$$

$$Cu_{1.96}S + 2\,Li^+ + 2\,e^- \rightarrow Li_2S + 1.96\,Cu \tag{7}$$

On charging from 1.5 to 2.0 V, djurleite appears again as can be seen Fig. 3 (f); but the peaks of Li_2S and Cu still remain. It is well-known that chalcocite (Cu_2S) or djurleite is transformed to a series of copper sulfides during oxidation i.e. digenite ($Cu_{1.8}S$), anilite (Cu_7S_4), blue covellite ($Cu_{1+x}S$, $x < 0.4$) and finally covellite [22,23]. Djurleite formed from the back reaction of (7) is converted to a series of copper sulfides which correspond to series of voltage plateaux
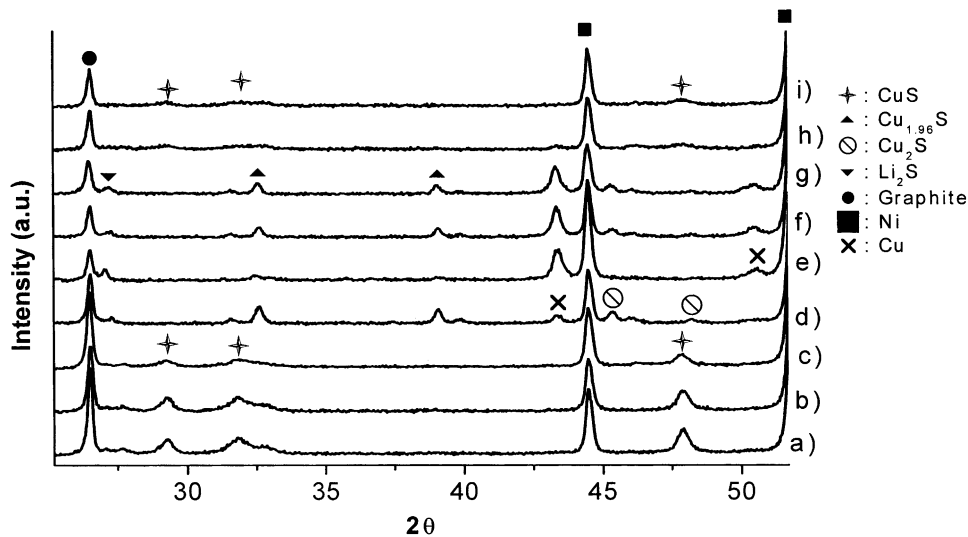

Fig. 3. XRD patterns of CuS electrode during the first cycle: (a) OCV; (b) discharge to 1.95 V; (c) discharge to 1.8 V; (d) discharge to 1.68 V; (e) discharge to 1.5 V; (f) charge to 2.0 V; (g) charge to 2.275 V; (h) charge to 2.45 V; (i) charge to 2.6 V.
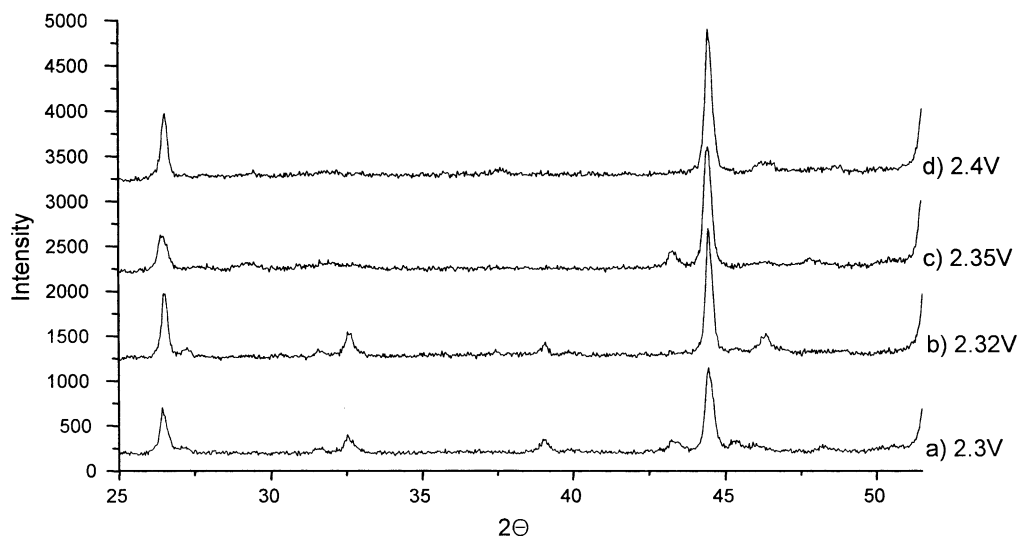
Fig. 4. XRD pattern of CuS electrode during charge reaction between 2.3 and 2.4 V for the first cycle: (a) 2.3 V; (b) 2.32 V; (c) 2.35 V; (d) 2.4 V.

between 2.3 and 2.4 V as shown in Fig. 2, as well as a series of peaks observed from EVS data in Fig. 1. Only digenite ($Cu_{1.8}S$) can be identified from the XRD patterns when the potential reaches to 2.32 V as can be seen in Fig. 4 (b). At 2.45 and 2.6 V (Fig. 3 (h) and (i)), where the charge reaction is finished, all the peaks have disappeared, but a broad CuS emerges with a low intensity. This suggests that during the charge reaction parts of the Cu and the Li_2S are changed to $Cu_{1.96}S$ which then returns to the original compound with a low conversion efficiency. This indicates that the first cycle reaction is not completely reversible.

As shown in Fig. 2, the capacity decreases rapidly within a few cycles. The major source of capacity fading is due to the irreversibility of reaction (7). Also, Li_2S formed during the first discharge reaction and Li_2S_x ($x > 1$, lithium polysulfide) are known to dissolve in the electrolyte [18,19]. Pure Li_2S powders (Aldrich >99.9%) were dissolved in 1 M $LiPF_6 + EC + 2EMC$ electrolyte, and the sulfur content in the electrolyte was measured using ion chromatography. The maximum solubility was found to be approximately 500 ppm in this electrolyte. The test cell was dissembled to

Table 1
Sulfur content (ppm) of electrolyte for each cycle analyzed by IC.

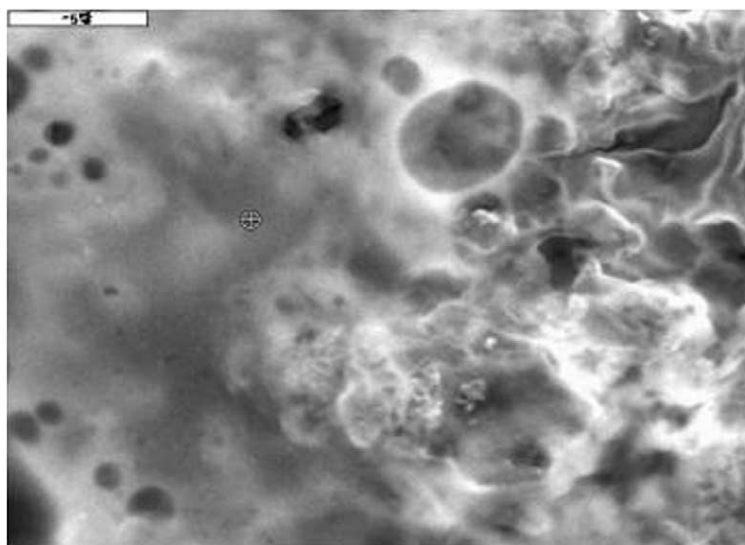| Cycle number	Sulfur content	
	Discharge	Charge
1	19	22
2	26	29
3	32	35
4	>40	>40
5	>40	>40

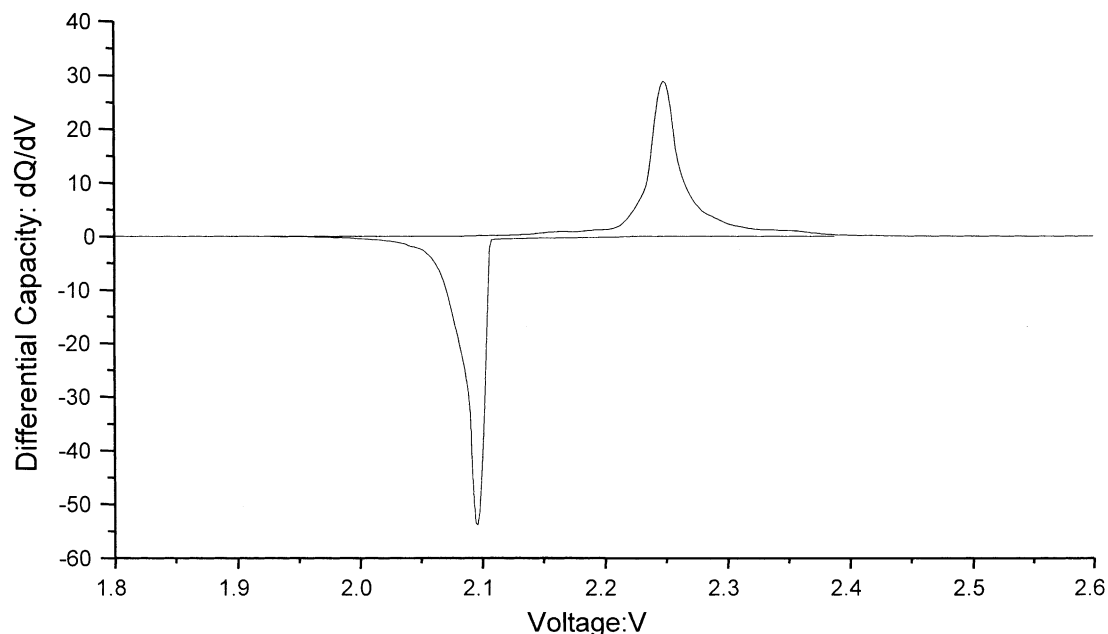Fig. 5. SEM micrograph of lithium anode surface after four cycles.

Fig. 6. EVS diagram cycled between 1.8 and 2.6 V.

measure the sulfur content in the electrolyte for each cycle, and the sulfur concentration was found increased with cycling as shown in Table 1. More than 20 wt.% of sulfur in the original CuS is dissolved after four cycles, which contributes to the irreversibility of the back reaction (7). The dissolved sulfur compounds migrate to the Li anode side through the membrane separator, and contaminate the Li anode as shown in Fig. 5. It has been reported [16,18] that the formation of S_8^- or polysulfide species in the Li/sulfur cell leads to a considerable loss of cathode material, as well as the corrosion of the Li anode by reacting with S_x^2 [16,18].

As mentioned above, the major capacity loss during cycling is due to the irreversibility of reaction (7) with

soluble Li_2S formation. If the potential range for cycling is limited between 2.6 and 1.8 V, it is expected that the cycleability can be enhanced with a high cycle efficiency. EVS data for a CuS electrode cycled between 1.8 and 2.6 V are shown in Fig. 6. It is seen the cell discharge capacity is 267 mAh^{-1} g (95% of theoretical capacity; 280 mAh^{-1} g), and the charge capacity is 232 mAh^{-1} g (83% of theoretical capacity, and 86% of discharge capacity). The reversibility of the cell reaction is fairly good.

XRD patterns for a CuS electrode in the same electrolyte cycled between 2.6 and 1.8 V are presented in Fig. 7. The patterns do not change during cycling which indicates that the reaction (5) is highly reversible. The cycle behavior of
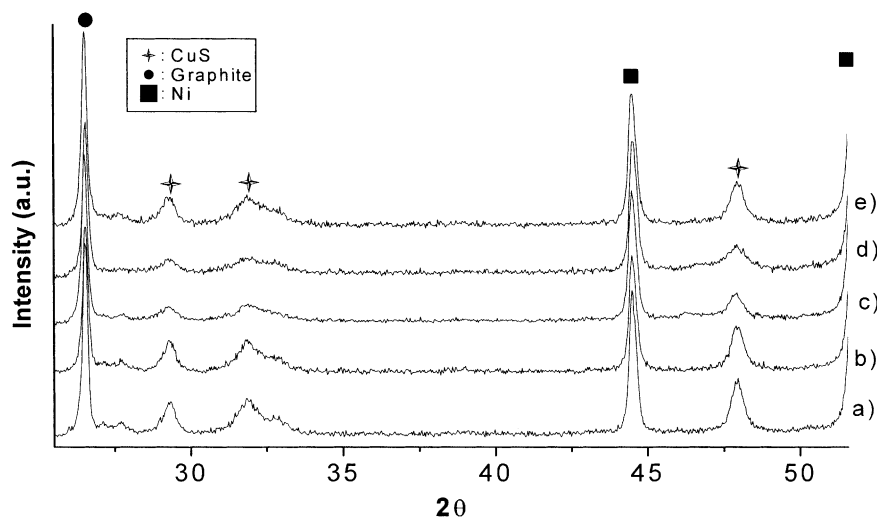

Fig. 7. XRD pattern of CuS electrode during cycling between 1.8 and 2.6 V: (a) OCV; (b) discharge to 1.95 V; (c) discharge to 1.8 V; (d) charge to 2.45 V; (e) charge to 2.6 V.
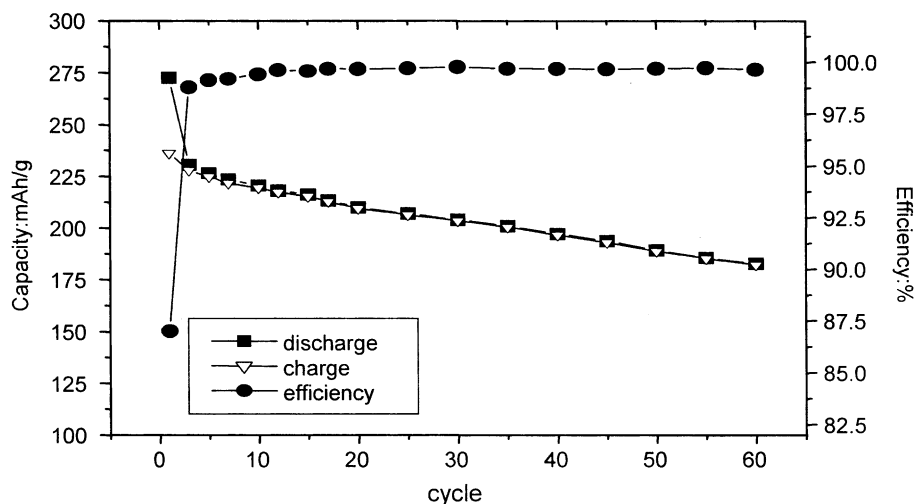
Fig. 8. Cycling behaviors of Li/CuS cell cycled in 1.8–2.6 V range.

the CuS electrode is shown in Fig. 8. The capacity is maintained at more than 70% of the initial value over 60 cycles, and the cycle efficiency remains above 99%.

4. Conclusions

The electrochemical behaviors of CuS electrode is studied systematically, and the failure mechanism is elucidated. The system has high capacity (520 mAh^{-1} g) with a two-stage reaction, which leads to two voltage plateaux in voltage profile. The second plateau reactions are not reversible which is partially due to the formation of soluble Li_2S. This is the main cause of the poor cycling behavior when cycling between 2.6 and 1.5 V. Based on the cell failure mechanism, cycling the electrode between 1.8 and 2.6 V greatly enhances the cyclealability. The capacity is maintained at more than 70% of the initial value and the cycle efficiency remains above 99% over 60 cycles due to the stability of the original crystalline phase, as confirmed by XRD.

References

[1] A. Attewell, P. Tattershall, in: Proceedings of the 29th Power Sources Symposium of the Electrochemical Society, Pennington, New Jersey. 1980, pp. 53–56.

[2] L.W. Langrish, in: Proceedings of the 29th Power Sources Symposium of the PSC Publication Committee, Red Bank, New Jersey,1969, pp. 67–69.

[3] D. Linden, N. Wilburn, E. Brooks, in: Proceedings of the 8th International Power Sources Symposium, Paper no. 20, Brighton, 1972.

[4] R.J. Jasinski, Electroanal. Chem. 26 (1970) 189.

[5] J.P. Gabano, V.L. Dechenaux, G.M. Gerbier, J. Jammett, Electrochem. Soc. 114 (1972) 489.

[6] A.J. Cuesta, D.D. Bump, in: B. Owens, N. Margalit (Eds.), Proceedings of the Symposia on Power Sources on Biomedical Implantable Applications and Ambient Temperature Lithium Batteries, The Electrochemical Society, Princeton, New Jersey, 1980, pp. 95–100.

[7] A.M. Bredland, T.G. Messing, J.W. Paulson, in: Proceedings of the 29th Power Sources Symposium of the Electrochemical Society, Pennington, New Jersey, 1980, pp. 82–85.

[8] K. Okamoto, S. Kawai, Jpn. J. Appl. Phys. 12 (1973) 1130.

[9] A. Etienne, J. Electrochem. Soc. 117 (1970) 870.

[10] N. Margalit, in: Gross (Ed.), Proceedings of the Symposium on Battery Design and Optimization of The Electrochemical Society, Princeton, New Jersey, 1979, pp. 320–326.

[11] F.W. Dampier, J. Electrochem. Soc. 121 (1974) 656.

[12] G. Eichinger, J.O. Besenhard, J. Electroanal. Chem. 72 (1976) 1–31.

[13] G. Eichinger, H.P. Fritz, Electroch. Acta 20 (1975) 753.

[14] R. Fournie, R. Messina, J. Perichon, J. Appl. Electrochem. 9 (1979) 329.

[15] D.P. Johnson, in: Proceedings of 29th Power Sources Symposium of the Electrochemical Society, Pennington, New Jersey, 1980, pp. 89–95.

[16] M. Hughes, N.A. Hampson, S. Karunathilaka, J. Power Sources 12 (1984) 144.

[17] I. Exner, J. Hep, J. Power Sources 12 (1984) 153.

[18] R. D Rauh, K.M. Abraham, G.F. Pearson, J.K. Surprenat, S.B. Brummer, J. Electrochem. Soc. 126 (1979) 523.

[19] E. Peled, A. Gorenshtein, M. Segal, Y. Sternberg, J. Power Sources 26 (1989) 269.

[20] D. Jensen, H. Pinhack, A. Reichert, GIT Fachz. Lab. (German) April (1996) 404–408.

[21] B. Divjak, W. Goessler, J. Chromatogr. A 884 (1/2, 4) (1999) 161–169.

[22] D.J. Vaughan, J.R. Craing, Mineral Chmistry of Metal Sufides, Cambridge University Press, Cambridge, 1978, pp. 209–292.

[23] P.J. Marcantonio, Chalcocite Dissolution in Acidic Ferric Sulfate Solutions, PhD Dissertation, University of Utah, Salt Lake City, Utah, 1976.